Environ Sci Pollut Res (2016) 23:15852–15861
DOI 10.1007/s11356-015-4330-0

INTERNATIONAL CONFERENCE ON INTEGRATED MANAGEMENT OF THE ENVIRONMENT - ICIME 2014

Improvement of oxygen-containing functional groups on olive stones activated carbon by ozone and nitric acid for heavy metals removal from aqueous phase

Thouraya Bohli[1] · **Abdelmottaleb Ouederni**[1]

Received: 15 December 2014 / Accepted: 5 March 2015 / Published online: 21 March 2015

Abstract Recently, modification of surface structure of activated carbons in order to improve their adsorption performance toward especial pollutants has gained great interest. Oxygen-containing functional groups have been devoted as the main responsible for heavy metal binding on the activated carbon surface; their introduction or enhancement needs specific modification and impregnation methods. In the present work, olive stones activated carbon (COSAC) undergoes surface modifications in gaseous phase using ozone (O_3) and in liquid phase using nitric acid (HNO_3). The activated carbon samples were characterized using N_2 adsorption–desorption isotherm, SEM, pHpzc, FTIR, and Boehm titration. The activated carbon parent (COSAC) has a high surface area of 1194 m^2/g and shows a predominantly microporous structure. Oxidation treatments with nitric acid and ozone show a decrease in both specific surface area and micropore volumes, whereas these acidic treatments have led to a fixation of high amount of surface oxygen functional groups, thus making the carbon surface more hydrophilic. Activated carbon samples were used as an adsorbent matrix for the removal of Co(II), Ni(II), and Cu(II) heavy metal ions from aqueous solutions. Adsorption isotherms were obtained at 30 °C, and the data are well fitted to the Redlich–Peterson and Langmuir equation. Results show that oxidized COSACs, especially COSAC(HNO_3), are capable to remove more Co(II), Cu(II), and Ni(II) from aqueous solution. Nitric acid-oxidized olive stones activated carbon was tested in its ability to remove metal ions from binary systems and results show an important maximum adsorbed amount as compared to single systems.

Keywords Surface modification · Oxygen functional groups · Olive stones activated carbon · Heavy metals · Adsorption

Nomenclature

COSAC	Olive stones activated carbon prepared by chemical activation using phosphoric acid
COSAC(HNO_3)	Oxidized olive stones activated carbon with nitric acid
COSAC(O_3)	Oxidized olive stones activated carbon with ozone
Ox-COSAC	Oxidized olive stones activated carbon
ICP-AES	Inductively coupled plasma atomic emission spectrometry
FTIR	Fourier transformed infrared spectroscopy
SEM	Scanning electron microscope
A, B	Redlich–Peterson parameters (L/g) and $(L/mol)^{\beta}$
q	Adsorption amount (mmol/g)
q^{binary}	Adsorption uptake from binary system (mmol/g)
q^{single}	Adsorption uptake from single solution (mmol/g)
K_F	Freundlich parameter $(mmol/L)(L/g)^{(1/n)}$
n	Freundlich constant
C	Liquid phase concentration of metal ion concentration (mmol/L)
K_L	Langmuir parameter (L/mmol)
m	The mass of adsorbent (g)
V	Volume of metal ion solution (L)

Responsible editor: Philippe Garrigues

✉ Thouraya Bohli
bohlithouraya@gmail.com

Abdelmottaleb Ouederni
mottaleb.ouederni@enig.mu.tn

[1] Laboratory of Research: Process Engineering and Industrial Systems (LR11ES54), National School of Engineers of Gabes, University of Gabès, 6026 Gabès, Tunisia

Greek letters

β Redlich–Peterson constant

Subscripts

E	Equilibrium
exp	Experimental value
cal	Value calculated by the model
s	Sips model
maxs	Maximum adsorbed quantity
PZC	Point of zero charge
ts	At time, t (min)
tots	Total adsorbed
0	Initial

Introduction

Nowadays, water pollution has been the major challenge to environmental researchers due to the release of different types of hazardous pollutants from various chemical industries. Heavy metals are the main pollutants that raise particular concern. Among various heavy metals, copper, nickel, and cobalt are non-biodegradable, hazardous, toxic, carcinogenic, and can cause illness in humans and can be fatal even at diluted concentrations (Kawarada et al. 2005). Several methods have been used for heavy metal removal such as chemical precipitation, ion exchange, membrane filtration, electrolytic method, coagulation, reverse osmosis, and adsorption (Fu and Wang (2011); Vitela-Rodriguez and Rangel-Mendez (2013)). Among these processes, the most promising efficient technique has been identified as adsorption with a suitable adsorbent. Porous activated carbon is one of the most widely used adsorbents for heavy metal removal from water and wastewaters; thanks to its higher performance related to physical and chemical properties such as surface area, pore volume, pore size distribution, and surface functional groups (Kasnejad et al. 2012; Bohli et al. 2015). Texture characteristics of porous carbon could be controlled by activation conditions (activation agent, temperature, and time), precursor, etc. The surface chemical functional groups were mainly derived from activation process, precursor, heat treatment, and post-chemical treatment (Ceyhan et al. 2013). Heavy metal adsorption investigated on modified activated carbon indicated that the adsorbed amount of metal ions depends strongly on the nature and quantity of acid–base functionalities (Biniak et al. 1999; Bansal and Goyal 2005; Zhang et al. 2015). It was devoted by some researches that oxygen functional groups, mainly acid ones, play an important role in cations binding on the activated carbon surface (Li et al. 2003; Zhang et al. 2005; Brasquet et al. 2002). An activated carbon with the highest amount of carboxylic function and with the lower pH_{pzc} adsorbs more heavy metals (Brasquet et al. 2002). Surface chemistry could be modified by various methods, such as acid treatment, oxidization, plasma, and microwave treatment. Oxidation is one of the most conventional modification technique used to induce or enhance oxygen functional groups on the surface of activated carbon such as carboxylic, lactones, phenols, ketones, quinones, hydroxyl, and carboxylic anhydride (Bansal and Goyal 2005), it can also remove the mineral elements and improve the hydrophilic of surface (Shen et al. 2008). These acidic surface groups are polar and enhance the ion exchange properties of the carbon, thereby increasing the adsorption of cation (Bansal and Goyal 2005). Oxidation of activated carbon can be performed in gaseous phase (dry oxidation) or in liquid phase (wet oxidation). In dry oxidation, an oxidizing gas such as stream, nonthermal plasma oxygen (Zhang et al. 2015), carbon dioxide (CO_2), and ozone (O_3) (Kohl et al. 2009; Valdés et al. 2002; Sivaraju and Begum 2013) are used. While in wet oxidation, liquid oxidizing agents such as hydrogen peroxide (H_2O_2) (Garcia et al. 2004), chloridric acid (HCl) (Wang and Zhu 2007), sulfuric acid (H_2SO_4) (Alvarez-Merino et al. 2005), and nitric acid (HNO_3) (Jia and Thomas 2000) are applied. Many publications have been interested in the oxidation of activated carbons using HNO_3 or ozone (Pereira et al. 2003; Machida et al. 2005; Lo et al. 2012; Kohl et al. 2009; Valdés et al. 2002; Sivaraju and Begum 2013). The treatment of activated carbon by ozone can reduce the specific surface area and modify the chemistry of carbon surface by enhancing or/and introducing selective functional groups able to react with metal ions. Ozone is a powerful oxidizing agent, which oxidizes the carbon surface to acidic functional groups such as carboxyl, lactone, anhydride, and phenol groups (Kohl et al. 2009; Valdés et al. 2002). Although the activated carbon surface can be oxidized with aqueous ozone, this process is far less effective than gaseous ozone treatments due to the low solubility of ozone in water (Rivera-Utrilla et al. 2011). Nitric acid aqueous phase treatment can induce an increase in carboxylic, quinone, and phenolic amounts (Jia and Thomas 2000). Most of these researchers were interested to the preparations and characterization of treated activated carbons, and only few ones were with application of nitric acid or ozone-treated activated carbons for heavy metal removal from aqueous phase (Li et al. 2003).

In this study, micropore olive stones activated carbon chemically activated was used as started material for posttreatments using gaseous ozone and nitric acid aqueous solution. Produced AC samples were characterized using N_2 adsorption–desorption isotherm, SEM, pH_{pzc}, FTIR, and

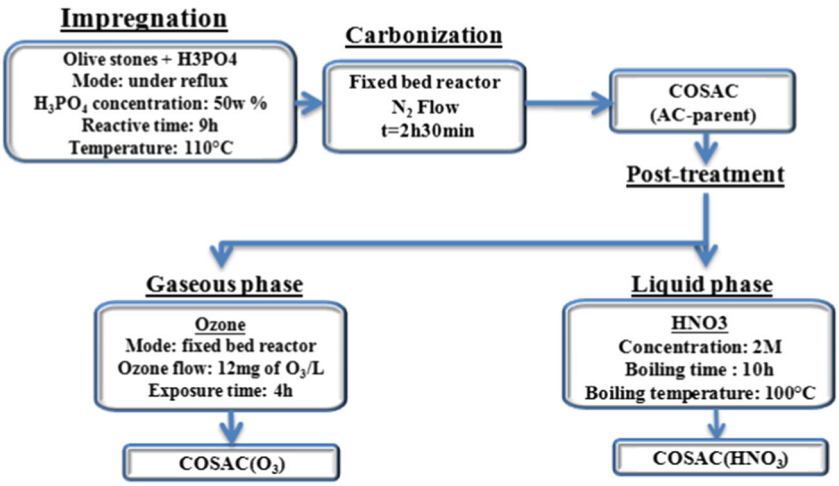

Fig. 1 COSACs preparation processes

Boehm titration and then evaluated its uses for copper, nickel and cobalt metal ions removal from single and binary aqueous solutions.

Material and methods

Materials

All the chemicals used in this study were of analytical grade. Stock solutions of metal ions were prepared by dissolving required amount of nitrate salt of cobalt nickel and copper metal in double distilled water. Metal ion concentrations were determined using an inductively coupled plasma–atomic emission spectrometer (ICP-AES; Activa-M, HORIBA Jobin Yvon) at wavelengths of 327.395, 238.892, and 231.604 nm for Cu(II), Co(II), and Ni(II), respectively. The detection limits of the analysis method were 2 μg/L for Cu(II), 5 μg/L for Co(II), and 5.5 μg/L for Ni(II).

Activated carbons preparations

Raw material "olive stones" were supplied from oleic industry from south Tunisia, and it was transformed on activated carbon chemically using H_3PO_4 according to the protocol optimized by Gharib and Ouederni (2005). Raw-milled olive stones were impregnated with a phosphoric acid solution (50 % by weight) at 110 °C for 9 h. After drying, the impregnated material was subjected to thermal activation at 410 °C for 2.5 h in a vertical tubular reactor feed by a stream of nitrogen and heated by electric furnace. The activated carbon obtained, labeled as COSAC, was washed thoroughly with distillate water to eliminate impurities, dried at 60 °C for 24 h and then sieved.

COSAC was used as started material or AC-parent for a posttreatment in liquid phase using nitric acid (HNO_3) and in gaseous phase using ozone (O_3) according to following oxidation protocols (Fig. 1):

- Oxidation of COSAC with HNO_3: The oxidation of COSAC was performed by boiling it with 2 M nitric acid solution concentration. A weight of 50 g of activated carbon was mixed with 500 mL of nitric acid solution for 10 h at about 100 °C in flask fitted with a reflux condenser. After oxidation, the samples was filtered, washed many times with distillated water, and then dried at 60 °C for 24 h. Obtained AC was named as COSAC(HNO_3).
- Oxidation of COSAC with O_3: The started material was oxidized with gaseous ozone in a fixed bed reactor loaded with 3 g of AC under a constant ozone flow of 12 mg of O_3/L of an air–ozone mixture, operating at room temperature and atmospheric pressure. Ozone was produced by a laboratory ozone generator and fed to the reactor for an exposure time of 4 h. After each treatment time, the carbon material was withdrawn from the reactor and washed and oven-dried for 12 h at 60 °C. Oxidized AC by ozone was labeled as COSAC(O_3).

Table 1 Surface functional groups of prepared COSACs (meq g^{-1})

AC	Carboxylic	Carbonyl	Lactone	Phenol	Total basic	pHpzc
COSAC	0.512	1.829	0.405	0.835	0.198	3.40
COSAC(O_3)	2.450	1.261	0.507	0.782	0.370	2.21
COSAC(HNO_3)	2.195	0.955	0.482	1.190	0.320	1.60

Activated carbons characterization

Nitrogen adsorption–desorption isotherms were measured using an automatic Sorptiometer Autosorb-1C Quantachrome apparatus at 77 K and in the range of relative pressure from 10^{-5} to 1.0. Total surface area was determined using the Brunauer–Emmett–Teller (BET) equation. The micropore diameter and micropore volume were calculated by the Dubinin–Radushkevich (DR) equation. SEM micrograph was carried out to show the pore structure of obtained activated carbons.

The point of zero charge was determined via batch equilibrium technique as following (Slobodan et al. 2007): a closed Erlenmeyer flask was filled with 50 mL of 0.01 M NaCl aqueous solution. The pH was adjusted to a given value between 2 and 12 by adding 0.1 M HCl or 0.1 M NaOH solutions. Then, a mass of 0.15 g of AC was added to a solution, and the final pH was measured after 48 h under agitation at room temperature. The intersection of the curve [($pH_{final} - pH_{initial}$) vs ($pH_{initial}$)] and the bisector gives the value pH_{pzc}.

FTIR spectrum was measured in the range of 500–4000 cm^{-1} using Bruker spectrophotometer model ALPHA with Platinum ATR Bruker adaptador.

Surface functional groups were determined by Boehm titration (Pereira et al. 2003). The Boehm titration method can be described as follows: 1 g of COSAC was placed in five Erlenmeyer flasks containing 50 mL of 0.1 M of HCl, NaOH, $NaHCO_3$, Na_2CO_3, and $NaOC_2H_5$ solutions, respectively. Then, the mixtures were agitated for 48 h. The suspensions were filtered through a 0.45-μm membrane filter, and the excess of base or acid was titrated with 0.1 M HCl or 0.1 M NaOH solutions, respectively. The amount of acidic groups on the activated carbon was calculated under the assumption that $NaOC_2H_5$ neutralizes carbonyl, carboxylic, lactones, and phenolic groups; NaOH, carboxylic, lactones, and phenolic groups; Na_2CO_3, carboxylic, and lactones; $NaHCO_3$, only carboxylic group. The number of surface basic sites is calculated from the amount of HCl that reacted with the carbon.

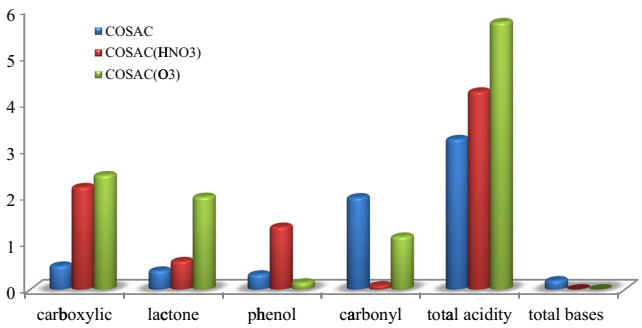

Fig. 2 Relative contents of surface functional groups of prepared COSACs

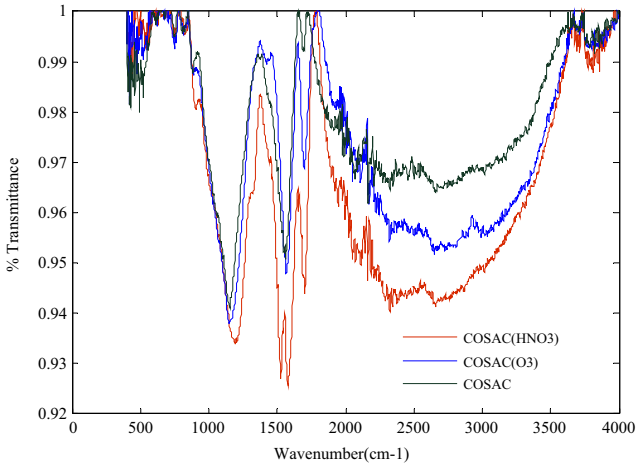

Fig. 3 FTIR spectra of prepared COSACs

Adsorption isotherms

The heavy metal ions (Co(II), Ni(II), and Cu(II)) adsorption capacities of COSAC, and ox-COSACs (COSAC(HNO) and COSAC(O_3)) were determined via batch mode in isothermal conditions at 30±2 °C and at pH 5. Fixed weight of AC samples of 0.3 g, with average particle size of 0.375 mm, were placed into 250-mL Erlenmeyer flasks containing 50 mL of metal ions solutions having different initial concentrations within the range of 0.5 to 5.0 mmol/L for Co(II), Ni(II), and Cu(II) metal ions at optimum pH value. The flasks were being agitated continuously during 10 h at 400 rpm. Then, the samples were filtrated through a 0.45-μm cellulose filter paper. After measurement of final pH, heavy metal samples are diluted with ultrapure

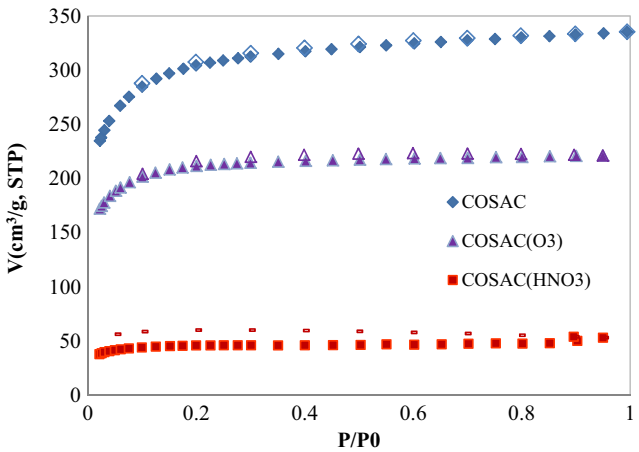

Fig. 4 N_2 adsorption–desorption isotherm at 77 K of untreated COSAC and ox-COSACs

Table 2 Physical properties of COSACs

AC	BET surface area ($m^2\ g^{-1}$)	DR micropore volume ($cm^3\ g^{-1}$)	Total volume ($cm^3\ g^{-1}$)	Pore diameter (A°)
COSAC	1194	0.552	0.561	20.72
COSAC(O_3)	797.4	0.342	0.343	17.21
COSAC(HNO_3)	173.2	0.079	0.082	19.01

water containing nitric acid to be ready for analysis by ICP-AES.

Experiments of binary adsorption isotherms were performed in the same conditions as single metal adsorption isotherms. The initial concentration of each metal ion varied from 0.5 to 5.0 mmol/L, while the concentration ratio was fixed and kept equal to the unit.

Each experiment was carried out in duplicate, and the average results are presented here. The adsorption capacities of activates carbons were calculated by using the following equation:

$$q = \frac{(C_0 - C_e)V}{m} \quad (1)$$

where q is the adsorption capacity (mg g^{-1}), V is the volume solution (L), C_0 is the initial metal ion concentration (mmol/L), C_e is the equilibrium metal ion concentration (mmol/L), and m is the mass of the activated carbon (g).

Results and discussion

Chemical characterization

Some functional groups occurred on the surface of COSAC and ox-COSACs were determined by Boehm titration. Results of surface functional groups reported in Table 1 indicate the predominance of acidic functional groups on the COSAC surface, especially carbonyl and phenol functional groups, resulting in 4.77 meq/g of total acidity. The use of phosphoric acid in the activation process provides a high amount of acid groups on the activated carbon surface, whereas total basicity accrues on COSAC surface was only 0.75 meq/g. Table 1 and Fig. 2 show the effect of oxidation treatment on the surface chemistry of COSAC. It is clear that nitric acid and ozone treatment generated an important increase in total acidic functional groups evaluated to be 4.235 and 5.720 meq/g, respectively, whereas basic sites are eliminated completely. It can be shown that the HNO_3 treatment mainly leads to an important increase of carboxylic and phenol, small increase in lactone groups, and a huge decease in carbonyl groups. While O_3 treatment leads to an important enhancement of both

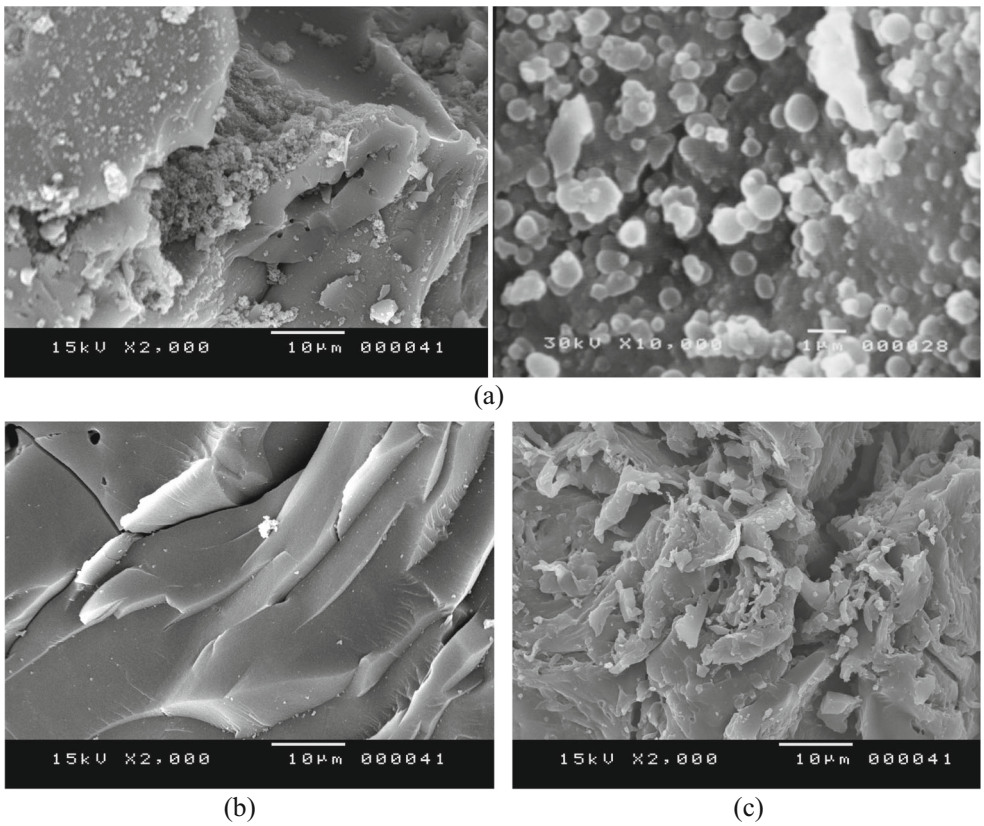

Fig. 5 Scanning electron micrographs of **a** COSAC, **b** COSAC(O_3), and **c** COSAC(HNO_3)

carboxylic and lactone groups and reduction of phenol and carbonyl groups as compare to the started material. The increase in acidity of ox-COSACs was proved by the measured decreased in pH_{pzc} values from 3.0 (for COSAC) to 2.21 and 1.20 for COSAC(HNO_3) and COSAC(O_3), respectively. Jaramillo et al. (2009) show that gaseous ozone treatment resulted in the fixation of acidic surface oxygen groups and the removal of basic surface oxygen groups and induced an decrease in the pH_{pzc} value from 8.8 for the untreated cherry stones activated carbon to 4.3 for the oxidized sample.

The surface chemistry characterization of COSAC, COSAC(HNO_3), and COSAC(O_3) was accomplished by FTIR spectroscopy (Fig. 3). The main components of the raw material olive stones are hemicellulose, cellulose, and lignin which has an aromatic character. The wide transmittance bands appear between 3772 and 3680 cm^{-1} are related to the O–H stretching vibration mode in alcohol and phenol. The region between 2921 and 2528 cm^{-1} is assigned to C–H stretching vibrations. The peak at 2325 cm^{-1} could be attributed to C=N stretching. Bands appear between 1622 and 1543 cm^{-1} are ascribed to C–C vibrations in aromatic rings (El-Hendawy 2006). The band appears at 1701 cm^{-1} denotes the existence of carboxyl groups. The bands between 1524 and 1580 indicates the presence of C=C ring stretching. The band between 1325 and 1456 cm^{-1} may be attributed to the aromatic CH and carboxyl–carbonate structures (Srivastava et al. 2006). The bands located at 1147 and 1198 cm^{-1} are related to C–O stretching vibrations in alcohols and phenols (Virote et al. 2005). The bands observed between 900 and 500 cm^{-1} are due to out of plane deformation mode of C–H for alkenes aromatic rings. Bands observed at 616 and 539 cm^{-1} are ascribed to C–H in out-of-plane bending in the edges of aromatic rings or are assigned to cyclic amides (El-Hendawy 2006). This behavior suggests that the activated carbon is mainly an aromatic polymer of activated carbon. The most important bands and peaks appearing on the spectrum of COSAC are the same presented on COSAC(O_3) and COSAC(HNO_3) but with high intensities. These results are in agreement with that found by Boehm titrations.

Textural characterization

The nitrogen gas adsorption–desorption isotherms of the COSAC and ox-COSACs at 77 K are given by Fig. 4. The isotherms appear to have a well-defined plateau and classified as Type I according to IUPAC classification. The N_2-isotherms show a small effect in desorption curves, especially in the case of COSAC(HNO_3), indicating the presence of mesopores with possible occurrence of capillary condensation phenomenon. The micropores and mesopores volumes were calculated (Table 2). From values listed in Table 1, one can observe that micropore volumes follow this trend: COSAC>COSAC(O_3)>COSAC(HNO_3). This order is consistent with the S_{BET} surface areas. The reduction in surface areas and pores volumes is may be due to porosity distraction and the blockage of some pores by oxygen groups, introduced by HNO_3 or O_3 treatments. Oxygen groups are probably fixed at the most active sites at the entrance of the micropores. Therefore, the access of nitrogen to these micropores becomes difficult, and as consequence, the pore volume is reduced and thus the specific surface area lowered. This is well visualized by SEM image determined for the three ACs. The SEM image of COSAC (Fig. 5a) shows that the microscopic shape of COSAC is an agglomeration of sub-micrometric particles. After nitric acid oxidation (Fig. 5b), the activated carbon presents a high

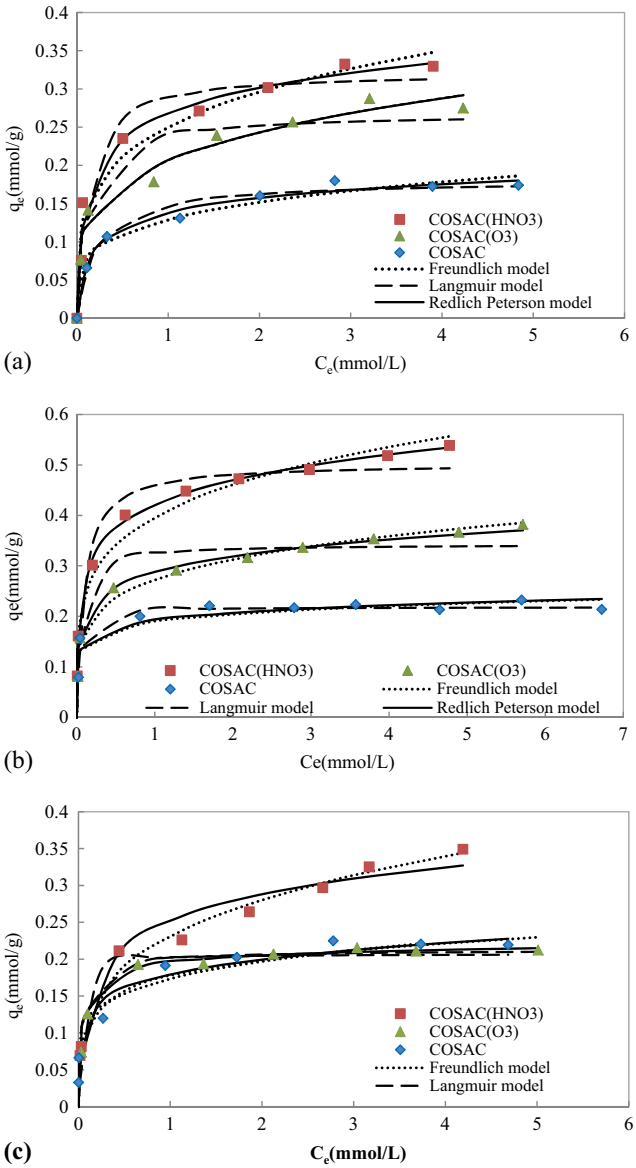

Fig. 6 Adsorption isotherms of **a** Co(II), **b** Ni(II), and **c** Cu(II) onto untreated and treated COSAC: *points* represent the experimental data, and *lines* represent modeling results by the Langmuir model (pH 5, equilibrium time 10 h, temperature 30 °C)

surface roughness. While ozone treatment results in softened texture and smooth surfaces in the form of parallel sheets (Fig. 5c), thereby pores are blocked by probable surface coalescence effects.

Results are in agreement with the studies of Gomez-Serrano et al. (2002), Park and Jin (2005), Kawamoto et al. (2005), and Sivaraju and Begum (2013). These researchers interpreted from their works that high ozone doses can destroy pore walls and fix large amounts of oxygen groups at the surface mainly carboxylic groups that make the carbon surface more hydrophilic.

Pereira et al. (2003), Machida et al. (2005), and Lo et al. (2012) observe from their studies that nitric acid treatment affect both chemical and textural properties of adsorbents. The oxidation destroyed the porous structure of the original AC by the loss of pore walls, also the total oxygen concentrations increased by the formation of acidic group, especially carbonyl, carboxyl, phenol, and nitrate groups.

Single heavy metal ions adsorption

The adsorption isotherms of Co(II), Ni(II), and Cu(II) onto COSAC, COSAC(HNO_3), and COSAC(O_3) were studied at 30 °C and an initial solution pH of 5. Adsorption isotherms data of the three heavy metal ions are reported in Fig. 6. The shapes of the isotherms are similar and show L-type behavior according to Giles classification (Giles et al. 1974) but differ in the amount of metal adsorbed. The shape of isotherms shows substantial affinity between the ACs surface and the three heavy metal ions, especially for copper and weaker competition with the solvent molecular. The removal of each metal ion increased with the initial metal concentration while the metal removal efficiency decreased which was known as the loading effect, describing the extent to which the total number of adsorption sites is occupied by the adsorbate (Prasad et al. 2008).

Obtained experimental adsorption data are fitted with Langmuir, Freundlich, and Redlich–Peterson models. The Langmuir equation can be presented as follows:

$$q_e = \frac{q_{max} K_L C_e}{1 + K_L C_e} \tag{2}$$

where C_e (mmol/L) is the equilibrium concentration metal ion in solution, q_e (mmol/g) is the surface concentration of metal ion at equilibrium, q_{max} (mmol/g) is the amount of metal ion adsorbed at complete monolayer coverage, and K_L (L/mmol) is a constant that relates to the heat of adsorption.

The Freundlich model is described by the following equation:

$$q_e = K_F C^n \tag{3}$$

where K_F (mmol/g (mmol/L)$^{-n}$) represents the adsorption capacity when metal ion equilibrium concentration (C_e) equals 1; n represents the degree of dependence of adsorption on equilibrium concentration.

The Redlich–Peterson model is given by the following equation:

$$q_e = \frac{A C_e}{1 + B C_e^{\beta}} \tag{7}$$

where A (L/g), B (L/mmol)$^{\beta}$, and β are the Redlich–Peterson constants.

For experimental equilibrium data fitting by Langmuir, Freundlich, and Redlich–Peterson models of the adsorption

Table 3 Calculated Langmuir, Freundlich, and Redlich–Peterson constants and correlation coefficients for the adsorption of Co(II), Ni (II), and Cu(II) onto COSAC and ox-COSAC

AC		COSAC			COSAC(O_3)			COSAC(HNO_3)		
Model metal ion		Co(II)	Ni(II)	Cu(II)	Co(II)	Ni(II)	Cu(II)	Co(II)	Ni(II)	Cu(II)
	q_{exp} (mg/g)	10.250	12.914	14.160	16.200	12.44	17.907	14.077	20.486	34.163
	q_{exp} (mmol/g)	0.174	0.220	0.223	0.275	0.212	0.382	0.329	0.349	0.538
Langmuir	K_L (L/mmol)	4.435	4.120	38.752	7.726	16.386	17.174	8.386	19.711	10.572
	q_{max} (mmol/g)	0.180	0.234	0.218	0.268	0.212	0.342	0.322	0.335	0.503
	R^2	0.991	0.987	0.965	0.940	0.994	0.956	0.964	0.997	0.978
Freundlich	K_F (mmol/L)(L/g)$^{(1/n)}$	0.129	0.171	0.188	0.205	0.177	0.272	0.250	0.231	0.396
	n	4.347	5.580	8.964	4.072	6.238	5.007	4.128	3.584	4.599
	R^2	0.960	0.979	0.904	0.978	0.947	0.989	0.968	0.992	0.984
Redlich–Peterson	A (L/g)	1.382	66.502	82.502	2.123	4.189	15.301	4.755	3.601	18.209
	B (L/mmol)$^{\beta}$	8.991	37.648	42.129	27.773	20.418	52.236	16.763	13.289	42.234
	β	0.882	0.845	0.897	0.757	0.964	0.863	0.867	0.853	0.858
	R^2	0.991	0.984	0.977	0.932	0.997	0.998	0.980	0.983	0.998

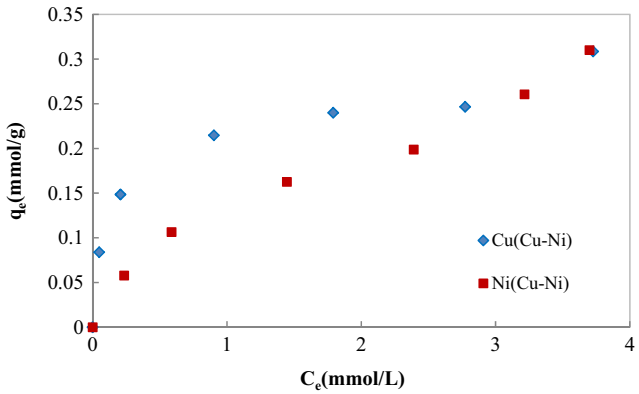

Fig. 7 Binary adsorption of Cu(II) and Ni(II) onto $COSAC_{(HNO3)}$ (pH 5; t_{eq}, 10 h; *T*, 30 °C; *dp*, 0.375 mm)

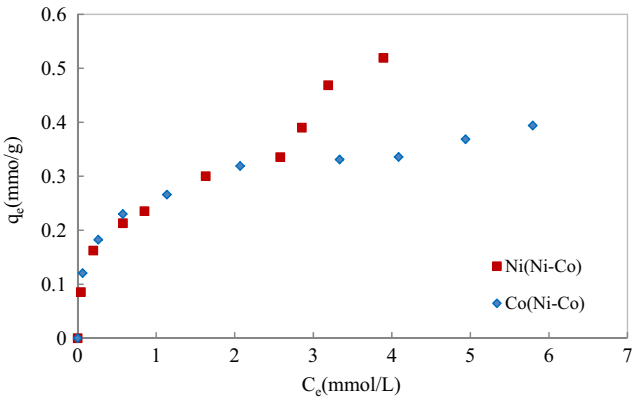

Fig. 9 Binary adsorption of Ni(II) and Co(II) onto $COSAC_{(HNO3)}$ (pH 5; t_{eq}, 10 h; *T*, 30 °C; *dp*, 0.375 mm)

of Co(II), Ni(II), and Cu(II) onto COSAC and ox-COSACs, we use the nonlinear regression via Solver which is an add-in in Microsoft Excel Office (Fig. 6). Identified model parameters and correlation coefficients (R^2) are reported in Table 3.

It is shown from Fig. 6 and Table 3 that Redlich–Peterson model fits the best to all the experimental data with highest correlation coefficients ($0.977 \leq R^2 \leq 0.998$) as compared to the other models except the adsorption isotherm of Ni(II) onto $COSAC(HNO_3)$ which was perfectly described by Freundlich model. Furthermore, the theoretical maximum values of the adsorption capacity of ACs given by Langmuir equation (q_{max}) were comparable to experimental measured values (Table 3), thus Redlich–Peterson and Langmuir model can perfectly describe the adsorption behavior of Co(II), Ni(II), and Cu(II) onto COSAC and ox-COSACs. The value of the maximum adsorption capacity determined by Langmuir model was found to increase in the order Co(II)<Ni(II)<Cu(II) and this for the COSAC and $COSAC(HNO_3)$, while for $COSAC(O_3)$, the adsorption order in terms of maximum adsorption follows this trend: Ni(II)<Co(II)<Cu(II). Results show that Cu(II) was found to be the most adsorbed metal onto the COSAC and ox-COSACs, the same results were found by Gao et al. (2009). For Co(II) and Ni(II), the change in the adsorption order cannot be related to the texture properties of the adsorbents and not also to the ionic radius of metal ions but one can explain this change by the difference in affinity between the metal ion in aqueous phase and the functional groups on activated carbon surfaces. Thus, Ni(II) can have a high relative affinity to phenol groups rather than carboxylic groups, this can be supported by the small "*n*" calculated values of Freundlich model (n=3.584) that suggests favorable adsorption of the Ni(II) metal ions onto $COSAC(HNO_3)$.

Although there is decrease in their specific surface areas, both ox-COSACs show important adsorption capacity toward metal ions studied compared to COSAC; this is mainly due to the enhancement of the amount of acid functional groups. Despite the higher acidic content functional groups presented on $COSAC(O_3)$ surface, $COSAC(HNO_3)$ shows higher adsorption of Co(II), Cu(II), and Ni(II) metal ions (Table 3). This can be due to the introduction of more phenol and carboxylic functional groups on $COSAC(HNO_3)$ surface. The adsorption amount determined by $COSAC(HNO_3)$, with lower pH_{pzc}, increased for more than 1.5 times as compared to the unmodified COSAC. This important increase in adsorbed quantity can be explained by the intervention of ion exchange mechanism. Moradi et al. (2011) compared the adsorption of Cu(II) ions onto two adsorbent SWCNTs and SWCNT-COOH. Although these two adsorbents have the same surface area (400 m^2/g), percentages removal of all metal ions studied

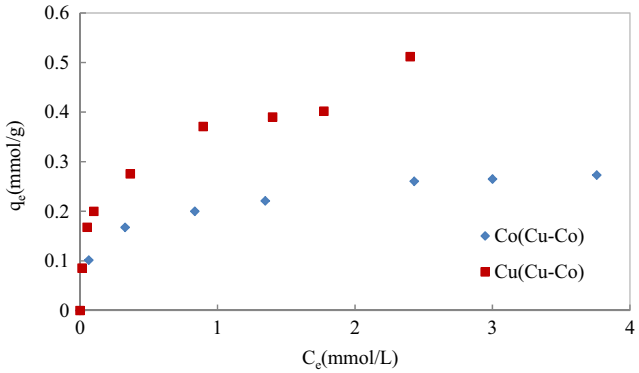

Fig. 8 Binary adsorption of Cu(II) and Co(II) onto $COSAC_{(HNO3)}$ (pH 5; t_{eq} 10 h; *T*, 30 °C; *dp*, 0.375 mm)

Table 4 Comparison equilibrium adsorption capacity, q_e(mmol/g), between single and binary adsorptions

Binary systems	$q_{e,1}^{single}$	$q_{e,1}^{binary}$	$q_{e,1}^{binary}/q_{e,1}^{single}$	$q_{e,2}^{single}$	$q_{e,2}^{binary}$	$q_{e,2}^{binary}/q_{e,2}^{single}$	$q_{e,\,tot}$ (mmol/g)
Ni(II)–Co(II)	0.226	0.335	1.482	0.329	0.317	0.963	0.652
Cu(II)–Co(II)	0.538	0.402	0.747	0.329	0.274	0.833	0.676
Cu(II)–Ni(II)	0.538	0.422	0.784	0.226	0.301	1.332	0.723

determined by SWCNT-COOH are very high as compared to SWCNTs. In the case of copper adsorption on activated carbon oxidized with HNO_3, Goyal et al. (2001) found that the adsorption removal was increased by a factor of about 3. Gao et al. (2009) reported that ion exchange and redox properties of CNTs-ox (both related to functional groups) play the main important role on the removal of studied metal ions. Girgis et al. (2007) reported that when an activated carbon is placed in aqueous solution, the acidic surface groups, present on the carbon surface, undergo ionization producing H^+ ions that are directed toward the liquid phase leaving the carbon surface with negatively charged sites. The larger the number of acidic groups on the carbon surface, the greater will be the negative charge on the carbon surface. This enhances the electrostatic attractive interactions between the negatively charged carbon surface and the positively charged metal cations.

Binary equilibrium adsorption results

Since single toxic metal species rarely exists in natural water and wastewater, it is therefore more important to study and evaluated ox-COSACs in the binary or the multi-solute adsorption.

Binary adsorption of Co(II), Ni(II), and Cu(II) onto COSAC and COSAC(HNO_3) was carried out by varying initial metal ions concentrations from 0.50 to 5.00 mmol/L and keeping the same concentration ratio (C_{0i}/C_{0j}) equal to 1.

From the analysis of equilibrium data given in Figs. 7, 8, and 9, it can be seen that adsorption isotherms for Co(II), Ni(II), and Cu(II) from binary Cu(II)-Ni(II), Cu(II)-Co(II), and Ni(II)-Co(II) aqueous systems onto $COSAC_{(HNO3)}$ showed a change in the shape as compared to single metal ions adsorption isotherms. Maximum adsorbed amounts of each metal from single and binary systems are measured and collected in Table 4.

The effect of the ionic interactions on the adsorption of copper in binary solutions may be represented by the ratio of the maximum adsorption capacity for copper ion in the presence of cadmium or lead ions, q_e^{binary}, to the adsorption amount of the copper in mono-solution (single adsorption), q_e^{single}, such that for (Mohan and Singh (2002)):

- $\frac{q_e^{binary}}{q_e^{single}} > 1$: the adsorption is promoted by the presence of the second metal ions;
- $\frac{q_e^{binary}}{q_e^{single}} = 1$: no interaction exists between adsorption species;
- $\frac{q_e^{binary}}{q_e^{single}} < 1$: The adsorption is inhibited by the presence of the second metal ions.

For the adsorption of Ni(II) and Co(II) in binary systems onto COSAC(HNO_3), the ratios were higher than unity for Ni(II), indicating synergism; means that the adsorbed amounts of both metal ions in mixture are greater than that of the individual ion in single solution systems and became lower than unity for Co(II), indicating that the adsorption of Ni(II) was promoted by the presence of Co(II), while Co(II) removal was depressed by the presence of Ni(II) in solution.

For other binary systems: Cu(II)–Co(II) and Cu(II)–Ni(II), the values of $q_{e,2}^{binary}/q_{e,2}^{sole}$ were <1, indicating that the adsorption of Cu(II) was affected by the presence of Co(II) or Ni(II) in the binary solutions. This result is in agreement with results found by Zhang (2011) and Qin et al. (2006). For the three studied binary systems ((Ni(II)–Co(II)), (Cu(II)–Co(II)), and (Cu(II)–Ni(II)), the total adsorption capacities of metal ions onto COSAC(HNO_3) were calculated to be 0.652, 0.676, and 0.723 mmol/g, respectively. These obtained values are greater than the adsorption capacities of Ni(II), Co(II)), and Cu(II) in single system. This increase in the maximum uptake in binary systems as compared to single systems is due to the increases of the uptake of one or both metal ions in the binary system on the adsorbent. These results are compatible with the results of Hanzlik et al. (2004) and Zhang (2011). The investigation of the three binary mixture systems showed that the amounts adsorbed were in the order Cu(II)>Ni(II)>Co(II) at the same equilibrium concentration which is consistent with the trend detected for the single components.

Conclusion

Olive stone activated carbon produced by thermochemical process using phosphoric acid (COSAC) was used as started material for surface modification using nitric acid and ozone phase oxidizing agents. These modifications introduce oxygen-containing functional groups on the surface of the COSAC making the adsorbent more hydrophilic in nature and able to remove more Co(II), Cu(II), and Ni(II) from single aqueous solution as compared to the started material despite the decrease in the specific surface area. COSAC(HNO_3) was found to be the most favorable one since higher Co(II), Cu(II), and Ni(II) adsorbed amounts are observed by using nitric acid-modified activated carbon, and this is due to the existence of phenol and carboxylic groups. The test of COSAC(HNO_3) as adsorbent from binary solutions shows important adsorbed amounts of both metal species formed from the binary solution.

Acknowledgments Sorptiometric and ICP-AES measurements realized by the Common Service Research Unit (USCR) of ENIG, University of Gabes, Tunisia, were gratefully acknowledged. FTIR analysis done by the Mass Spectrometry Unit, Technical Research Services Science and Technology Park of the University of Girona Pic Paguera 15, Girona, Catalonia (Spain), was gratefully acknowledged.

Compliance with ethical standards This research does not involve any human or animal participants.

Conflict of interest The authors declare that they have no conflict of interest.

Funding This study was funded by the budget of our laboratory, Laboratory of Research: Process Engineering and Industrial Systems (LR11ES54). Authors agree with all terms of compliance with ethical standards (COPE guidelines).

References

Alvarez-Merino MA, Lopez-Ramon V, Moreno-Castilla C (2005) A study of the static and dynamic adsorption of Zn(II) ions on carbon materials from aqueous solutions. J Colloid Interface Sci 288:335–341

Bansal RC, Goyal M (2005) Activated carbon adsorption. ISBN 0-8247-5344-5

Biniak S, Pakuła M, Szymański GS, Świątkowski A (1999) Effect of activated carbon surface oxygen- and/or nitrogen-containing groups on adsorption of copper(II) ions from aqueous solution. Langmuir 18:6117–6122

Bohli T, Ouederni A, Fiol N, Villaescusa I (2015) Evaluation of an activated carbon from olive stones used as an adsorbent for heavy metal removal from aqueous phases. C R Chim 18:88–99

Brasquet CF, Reddad Z, Kadirvelu K, Cloirec P (2002) Modelling the adsorption of metal ions (Cu^{2+}, Ni^{2+} and Pb^{2+}) onto ACCs using surface complexation models. Appl Surf Sci 196:356–365

Ceyhan AA, Sahin O, Baytar O, Saka C (2013) Surface and porous characterization of activated carbon prepared from pyrolysis of biomass by two-stage produce at low activation temperature and it's the adsorption of iodine. J Anal Appl Pyrolysis 104:378–383

El-Hendawy ANA (2006) Variation in the FTIR spectra of a biomass under impregnation,carbonization and oxidation conditions. J Anal Appl Pyrolysis 75:159–166

Fu F, Wang Q (2011) Removal of heavy metal ions from wastewaters: a review. J Environ Manag 92:407–418

Gao Z, Bandosz TJ, Zhao Z, Han M, Qiu J (2009) Investigation of factors affecting adsorption of transition metals on oxidized carbon nanotubes. J Hazard Mater 167:357–365

Garcia T, Murillo R, Cazorla-Amoros D, Mastral AM, Linares-Solano A (2004) Role of the AC surface chemistry in the adsorption of phenanthrene. Carbon 42:1683–1689

Goyal M, Rattan VK, Aggarwal D, Bansal RC (2001) Removal of copper from aqueous solutions by adsorption on activated carbon. Colloid Surface 190:229–238

Gharib H, Ouederni A (2005) Récents Progrès en Génie des Procédés, ISBN 2-910239-66-7, Ed.SFGP, Paris-France 92

Giles CH, Smith D, Huitson A (1974) A general treatment and classification of the solute adsorption isotherm. I. Theoretical. J Colloid Interface Sci 47:755–765

Girgis BS, Attia AA, Fathy NA (2007) Modification in adsorption characteristics of activated carbon produced by H3PO4 under flowing gases. Colloids Surf A Physicochem Eng Asp 299:79–87

Gomez-Serrano V, Alvarez PM, Jaramillo J, Betran FJ (2002) Formation of oxygen complexes by ozonation of carbonaceous materials prepared from cherry stones. I. Thermal effects. Carbon 40:513–522

Hanzlik J, Jechlicka J, Sebek O, Weishauptova Z, Machovic V (2004) Multicomponent adsorption of Ag(I), Cd(II) and Cu(II) by natural carbonaceous materials. Water Res 38:2178–2184

Jaramillo J, Gomez-Serrano V, Alvarez PM (2009) Enhanced adsorption of metal ions onto functionalized granular ACs prepared from cherry stones. J Hazard Mater 161:670–676

Jia YF, Thomas KM (2000) Adsorption of cadmium ions on oxygen surface sites in activated carbon. Langmuir 16:1114–1122

Kasnejad MH, Esfandiari A, Kaghazchi T, Asasian N (2012) Effect of pre-oxidation for introduction of nitrogen containing functional on Cu(II) adsorption. J Taiwan Inst Chem Eng 43:736–740

Kawamoto K, Ishimaru K, Imamura Y (2005) Reactivity of wood charcoal with ozone. J Wood Environ 51:66–72

Kawarada K, Haneishi K, Iida T (2005) Wood Ind 60:398

Kohl S, Drochner A, Vogel H (2009) Quantification of oxygen surface groups on carbon materials via diffuse reflectance FT-IR spectroscopy and temperature programmed desorption. Catal Today 150:67–70

Li YH, Ding J, Luan Z, Di Z, Zhu Y, Xu C, Wu D, Wei B (2003) Competitive adsorption of Pb^{2+}, Cu^{2+} and Cd^{2+} ions from aqueous solutions by multiwalled carbon nanotubes. Carbon 41:2787–2792

Lo SF, Wang SY, Tsai MJ, Lin LD (2012) Adsorption capacity and removal efficiency of heavy metal ions by Moso and Ma bamboo activated carbons. Chem Eng Res Des 90:1397–1406

Machida M, Yanazaki R, Aikawa M, Tatsumoto H (2005) Role of minerals in carbonaceous adsorbents for removal of Pb (II) ions from aqueous solution. Sep Purif Technol 46:88–94

Mohan D, Singh KP (2002) Single-and multi-component adsorption of cadmium and zinc using activated carbon derived from bagasse—an agricultural waste. Water Res 36:2304–2318

Moradi O, Zare K, Yari M (2011) Interaction of some heavy metal ions with single walled carbon nanotube. Int J Nanotube Dimension 3:203–220

Park SJ, Jin SY (2005) Effect of ozone treatment on ammonia removal of ACs. J Colloid Interface Sci 286:417–419

Pereira MFR, Soares SF, Orfao JJM, Figueiredo JL (2003) Adsorption of dyes on ACs: influence of surface chemical groups. Carbon 41:811–821

Prasad M, Xu H, Saxena S (2008) Multi-component sorption of Pb(II), Cu(II) and Zn(II) onto low-cost mineral adsorbent. J Hazard Mater 154:221–229

Qin F, Wen B, Shan XQ, Xie YN, Liu T, Zhang SZ, Khan SU (2006) Mechanisms of competitive adsorption of Pb, Cu and Cd on peat. Environ Pollut 144:669–680

Rivera-Utrilla J, Sanchez-Polo M, Gomez-Serrano V, Alvarez PM, Alvim-Ferraz MCM, Dias JM (2011) Activated carbon modifications to enhance its water treatment applications: an overview. J Hazard Mater 187:1–23

Shen W, Li Z, Liu Y (2008) Surface Chemical Functional Groups Modification of Porous Carbon. Recent Pat Chem Eng 27:1874-4788

Sivaraju SS, Begum KMMS (2013) Performance of ozone treated rice husk carbon (OTRHC) for continuous adsorption of Cr (VI) ions from synthetic effluent. J Environ Chem Eng 1:79–85

Slobodan K, Ljiljana Cerovi S, Djuro Cokeša M, Zec S (2007) The influence of cationic impurities in silica on its crystallization and point of zero charge. J Colloid Interface Sci 309:155–159

Srivastava VC, Mall ID, Mishra IM (2006) Equilibrium modeling of single and binary adsorption of cadmium and nickel onto bagasse fly ash. Chem Eng J 117:79–91

Valdés H, Sánchez-Polo M, Rivera-Utrilla J, Zaror CA (2002) Effect of ozone treatment on surface properties of activated carbon. Langmuir 18:2111–2116

Virote B, Srisuda S, Wiwut T (2005) Preparation of activated carbons from coffee residue for the adsorption of formaldehyde. Sep Purif Technol 42:159–168

Vitela-Rodriguez AV, Rangel-Mendez JR (2013) Arsenic removal by modified activated carbons with iron hydro (oxide) nanoparticles. J Environ Manag 114:225–231

Wang S, Zhu ZH (2007) Effect of acidic treatment of activated carbons on dye adsorption. Dyes Pigments 75:306–314

Zhang M (2011) Adsorption study of Pb(II), Cu(II) and Zn(II) from simulated acid mine drainage using dairy manure compost. Chem Eng J 172:361–368

Zhang B, Xu P, Qiu Y, Yu Q, Ma J, Wu H, Luo G, Xu M, Yao H (2015) Increasing oxygen functional groups of activated carbon with non-thermal plasma to enhance mercury removal efficiency for flue gases. Chem Eng J 263:1–8